Available online at www.sciencedirect.com
SCIENCE DIRECT®
Journal of Nuclear Materials 334 (2004) 90–96
journal of nuclear materials
www.elsevier.com/locate/jnucmat

Stability evaluation of fluorite structure phase in PuO_2–UO_2–ZrO_2 system by thermodynamic modelling

Hajime Kinoshita *, Masayoshi Uno, Shinsuke Yamanaka

Department of Nuclear Engineering, Graduate School of Engineering, Osaka University, 2-1 Yamada-oka, Suita, Osaka 565-0871, Japan

Received 20 January 2003; accepted 5 April 2004

Abstract

A thermodynamic modelling was performed for PuO_2–UO_2–ZrO_2 system based on the data available in the literature to evaluate stability of the fluorite structure phase in PuO_2–UO_2–ZrO_2 system. The assessment of the heat capacity and phase diagram suggested that the deviation from the ideality in the PuO_2–UO_2 system is negligibly small. The calculated pseudo-ternary phase diagrams implied that the fluorite structure phase of PuO_2–ZrO_2 subsystem is more stable than that of UO_2–ZrO_2 subsystem in the lower temperature range and that the latter is more stable than the former in the higher temperature range. The effect of ZrO_2 dissolution to PuO_2 was larger both on the enthalpy and entropy of the fluorite structure phase than that to UO_2 in the low ZrO_2 composition range. On the other hand, UO_2 had a larger effect on the stability of the fluorite structure phase in the high ZrO_2 composition range.

PACS: 28.41.Bm; 28.41.Kw; 82.20.Wt; 82.60.Lf

1. Introduction

Such oxides as PuO_2 and UO_2 are well known materials relevant to nuclear fuel/waste industry, and these oxides can form solid solutions with monoclinic, tetragonal and fluorite structures by combining with ZrO_2 [1,2]. Knowledge of the phase equilibria of the solid solutions among these oxides is of great importance for the plutonium disposition, which is acknowledged as one of the most urgent issue at the world level for proliferation resistance [3]. Possible plutonium deposition scheme includes utilisation of plutonium in the nuclear reactors as mixed oxide fuel (MOX: PuO_2+UO_2) [4], rock-like oxide (ROX: PuO_2+ZrO_2/$MgAl_2O_4$) fuel [5], or solid solutions with inactive materials acting as a diluent to soften the high fission density and high fuel temperatures [6,7].

Phase stability of the fluorite structure phase in PuO_2–UO_2–ZrO_2 systems is of particular interest to the present study. Thermodynamic modelling was utilised to evaluate the stability of these systems based on the CALculation of PHAse Diagram (CALPHAD) technique [8]. As is also defined as computer coupling of phase diagrams and thermochemistry [8], this technique makes it possible to predict the phase behaviour in highly complex multi-component systems based on the thermodynamic properties such as the Gibbs energy of the components. This technique has been successfully applied for such systems as O–U–Zr [9] and O–Pu–Zr [1]. The CALPHAD technique has also been applied for such pseudo-binary systems as PuO_2–ZrO_2 [1] and UO_2–ZrO_2 [2,9].

In the first part of the study, thermodynamic modelling was performed to assess the thermodynamic parameters for PuO_2–UO_2 pseudo-binary system based on the phase diagram and heat capacity data. Using the

* Corresponding author. Current address: Department of Chemistry, Centre for Radiochemistry Research, University of Manchester, Oxford Road, Manchester M13 9PL, UK. Tel.: +44-161 275 1405.

E-mail addresses: hajime.kinoshita@man.ac.uk, khaji@stu.nucl.eng.osaka-u.ac.jp (H. Kinoshita).

0022-3115/$ - see front matter © 2004 Published by Elsevier B.V.
doi:10.1016/j.jnucmat.2004.04.322

assessed data for PuO_2–UO_2 together with those for the PuO_2–ZrO_2 [1] and UO_2–ZrO_2 [2] systems, a set of PuO_2–UO_2–ZrO_2 pseudo-ternary phase diagrams was also calculated. In the second part, the stability of the fluorite structure phases in the PuO_2–UO_2–ZrO_2 system was discussed with respect to the deviation from the ideality and partial molar quantities of the PuO_2–UO_2, PuO_2–ZrO_2 and UO_2–ZrO_2 pseudo-binary subsystems.

2. Thermodynamic modelling

2.1. Principle

Thermodynamic modelling was performed using the program POLY-3 included in Thermo-Calc [10]. The quantity stored in the data for the calculation is Gibbs energy of formation for phases, G (J/mol). In the PuO_2–UO_2–ZrO_2 system, four solution phases (monoclinic, tetragonal, cubic and liquid phases) are present. The Gibbs energy of a solution phase (both solid and liquid) applied in the present study consists of such terms as reference (G^{ref}), ideal (G^{id}) and excess (G^{xs}) Gibbs energies.

$$G = G^{ref} + G^{id} + G^{xs}, \tag{1}$$

where G^{ref} is the contribution of pure components of the phase to the Gibbs energy, G^{id} is the ideal mixing contribution, known as ideal entropy of mixing and G^{xs} is the contribution due to non-ideal interactions between the components, also known as excess Gibbs energy of mixing.

In the present study, Gibbs energies of the solution phases were expressed with the general multi-sublattice model proposed by Sundman et al. [11]. For example, in a simple case of a MO_2 phase with a formula (A, B)$_1$(C)$_2$, the reference (G^{ref}), ideal (G^{id}) and excess (G^{xs}) Gibbs energies are expressed as Eqs. (2)–(4), respectively.

$$G^{ref} = y_A^1 y_C^2 G_{AC}^0 + y_B^1 y_C^2 G_{BC}^0, \tag{2}$$

$$G^{id} = RT\left\{N^1\left(y_A^1 \log_e y_A^1 + y_B^1 \log_e y_B^1\right)\right\}, \tag{3}$$

$$G^{xs} = y_A^1 y_B^1 y_C^2 \left\{L_{A,B:C}^0 + L_{A,B:C}^1\left(y_A^1 - y_B^1\right) + L_{A,B:C}^2\left(y_A^1 - y_B^1\right)^2 + \cdots\right\}, \tag{4}$$

where y_i^s represents the site fraction of component 'i' on sublattice 's', G_{ij}^0 is the Gibbs energy of the pure 'ij' phase in question and N^s is the total number of the site on the sublattice 's'. L_{ij}^n are constants known as interaction parameters described by using Redlich–Kister type polynomial expression [12].

2.2. Data for PuO_2–UO_2–ZrO_2 system

Structure types and sublattice models of the phases used for the present calculation are summarised in Table 1 together with the reference for the Gibbs energy data. The monoclinic, tetragonal and cubic (fluorite) phases were all treated as solid solutions expressed with a formula (Pu, U, Zr)$_1$(O)$_2$. This model requires Gibbs energies of the three boundary compounds (Pu)$_1$(O)$_2$, (U)$_1$(O)$_2$ and (Zr)$_1$(O)$_2$ for each phase. Although the Gibbs energy for (Pu)$_1$(O)$_2$ and (U)$_1$(O)$_2$ with a fluorite structure is available from the SGTE (Scientific Group Thermodata Europe) database [13], those for the monoclinic and tetragonal structure phases are not. The Gibbs energies for these metastable phases were estimated in the same manner as applied for the ZrO_2–UO_2 [2] system using following equations:

Table 1
Phases in the PuO_2–UO_2–ZrO_2 pseudo-ternary system used in the present modelling

Phase	Structure	Sublattice model	Gibbs energy data
Alpha-ZrO_2	Monoclinic	(Pu, U, Zr)$_1$(O)$_2$	PuO_2: (Cubic-PuO_2) + 6.98693T [1] UO_2: (Cubic-UO_2) + 6.98693T [2] ZrO_2: taken from SGTE [13]
Beta-ZrO_2	Tetragonal	(Pu, U, Zr)$_1$(O)$_2$	PuO_2: (Cubic-PuO_2) + 1.18548T [1] UO_2: (Cubic-UO_2) + 1.18548T [2] ZrO_2: taken from SGTE [13]
PuO_2 UO_2 Gamma-ZrO_2	Cubic (fluorite)	(Pu, U, Zr)$_1$(O)$_2$	PuO_2: taken from SGTE [13] UO_2: taken from SGTE [13] ZrO_2: taken from SGTE [13]
Liquid		(Pu, U, Zr)$_1$(O)$_2$	PuO_2: taken from SGTE [13] UO_2: taken from SGTE [13] ZrO_2: taken from SGTE [13]

$$G(\text{Monoclinic-PuO}_2/\text{UO}_2) = G(\text{Cubic-PuO}_2/\text{UO}_2) + 6.98693T, \quad (5)$$

$$G(\text{Tetragonal-PuO}_2/\text{UO}_2) = G(\text{Cubic-PuO}_2/\text{UO}_2) + 1.18548T. \quad (6)$$

The Gibbs energies for the $(Zr)_1(O)_2$ with monoclinic, tetragonal and cubic (fluorite) structures were taken from the SGTE database [13]. The liquid phase was also expressed with a formula (Pu, U, $Zr)_1(O)_2$. The Gibbs energies for the boundary compositions $(Pu)_1(O)_2$, $(U)_1(O)_2$ and $(Zr)_1(O)_2$ for this model are available from the SGTE database [13].

The interaction parameters required for the present calculation were taken from the literature for PuO_2–ZrO_2 [1] and UO_2–ZrO_2 [2] pseudo-binary systems. The interaction parameters for the PuO_2–UO_2 system were assessed in the following section.

3. Results and discussion

3.1. PuO_2–UO_2 pseudo-binary system

Both PuO_2 and UO_2 form only a cubic (fluorite) structure phase up to their melting temperature. The ionic radii of Pu^{4+} and U^{4+} in the fluorite structure are very similar (Pu^{4+}: 0.096 nm, U^{4+}: 0.100 nm, [14]), and PuO_2 and UO_2 are totally miscible in the all composition range. Therefore, only a fluorite structure phase and a liquid phase appear in the PuO_2–UO_2 pseudo-binary system.

The ideality of the PuO_2–UO_2 system is unclear. Beauvy has studied PuO_2–UO_2 solid solution and shown a possibility of its deviation from the ideality [15]. That experimental study focuses on the solid solution in the low PuO_2 composition range (up to 20 mol% of PuO_2) and includes such thermodynamic property as specific heat up to 873 K. On the other hand, Carbajo et al. has mentioned in their very completed review on the thermophysical properties of MOX fuel that the solid solution in the PuO_2–UO_2 system is almost ideal [4]. They also recommended the calculation from the composition following the Neumann–Kopp rule for the determination of the specific heat of the PuO_2–UO_2 solid solution.

Fig. 1 compares the calculated heat capacity of PuO_2, UO_2 and $(Pu_{0.25}U_{0.75})O_2$ with the experimental data after Gibby et al. [16]. The calculation was performed by assuming that PuO_2 and UO_2 form an ideal solid solution. The calculated and experimental values show a very good agreement. Since heat capacity is the differentiation of enthalpy with respect to temperature ($C_p = \mathrm{d}H/\mathrm{d}T$), it implies that the interaction parameter for (Pu, U)O_2 has no or negligibly small temperature dependence. The deviation in the high temperature region is attributed to (i) an anomalous increase in the heat capacity of UO_2 [4,17] and (ii) the limitation in the PuO_2 data that is not well defined in high temperature [4].

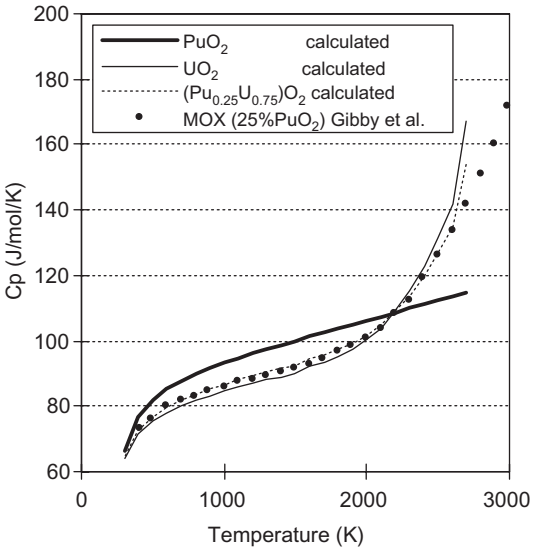

Fig. 1. Heat capacity of PuO_2, UO_2 and $(Pu_{0.25}U_{0.75})O_2$. The figure also indicates the experimental data after Gibby et al. [16] for comparison.

Fig. 2 compares the phase diagram calculated in the present work with that recommended in the literature [4] for the PuO_2–UO_2 system in the low PuO_2 composition range. The calculation was carried out with an assumption of that PuO_2 and UO_2 form ideal solid and

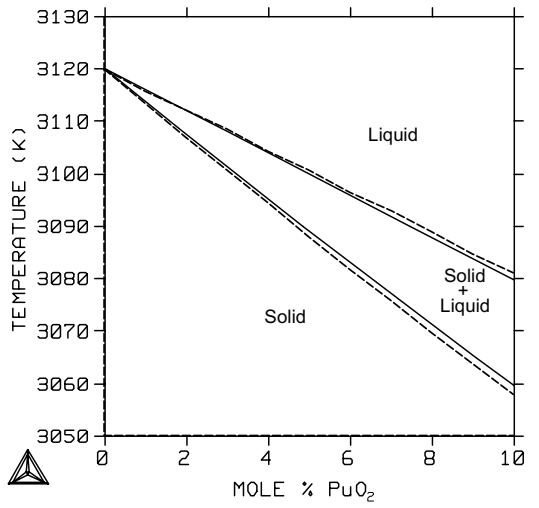

Fig. 2. Phase diagram for the PuO_2–UO_2 system in the low PuO_2 composition range: (—) calculated in the present work and (- - -) recommended in the literature [4].

liquid solutions. The calculated and recommended phase diagrams show a very good agreement even in the low PuO_2 composition range in which a possibility of deviation from the ideality was pointed out [15]. Therefore, we conclude that the deviation from the ideality in the PuO_2–UO_2 system is negligibly small and that it is reasonable to treat the phases in this pseudo-binary system as ideal solutions (the interaction parameters in this system are all zero).

3.2. PuO_2–UO_2–ZrO_2 pseudo-ternary phase diagram

Calculated phase diagrams for PuO_2–UO_2–ZrO_2 pseudo-ternary system are indicated in Fig. 3. In the lower temperature range up to about 1400 K, the system has only monoclinic and cubic (fluorite) phases at high and low ZrO_2 concentration, respectively. Significant amount of tetragonal phase appears at about 1450 K on the UO_2–ZrO_2 side, and the monoclinic phase disappears above this temperature. As temperature increases, the cubic phase region drastically expands and the cubic single-phase region becomes dominant in the system by the temperature of 1800 K. Finally, at 2600 K the system has the cubic single-phase in almost all composition range. These figures clearly indicate that cubic structure phase of the PuO_2–UO_2 is very stable. It is also implied that cubic structure phase of the PuO_2–ZrO_2 is more stable than that of the UO_2–ZrO_2 in the temperature range up to 2600 K.

Fig. 4 indicates calculated phase diagrams of the system in the higher temperature range. Since melting temperature of PuO_2 was about 2650 K with the data used in the present calculation, the system has certain amount of liquid phase at 2700 K in the high PuO_2 concentration region. As temperature increases, the liquid phase region expands towards high ZrO_2 concentration region as observed in the phase diagram at 2800 K. The cubic phase on the UO_2–ZrO_2 side starts melting at around 2850 K and the system has two cubic phase regions at 2900 K. The system has the liquid phase in almost all composition range at 3000 K except high UO_2 concentration region. The cubic phase finally vanishes at 3100 K. It is implied that cubic structure phase of the UO_2–ZrO_2 is more stable than that of the PuO_2–ZrO_2 in the temperature range above 2700 K.

3.3. Stability of fluorite structure phase

Fig. 5 compares the excess Gibbs energies of cubic (fluorite) phases for the PuO_2–UO_2, PuO_2–ZrO_2 and

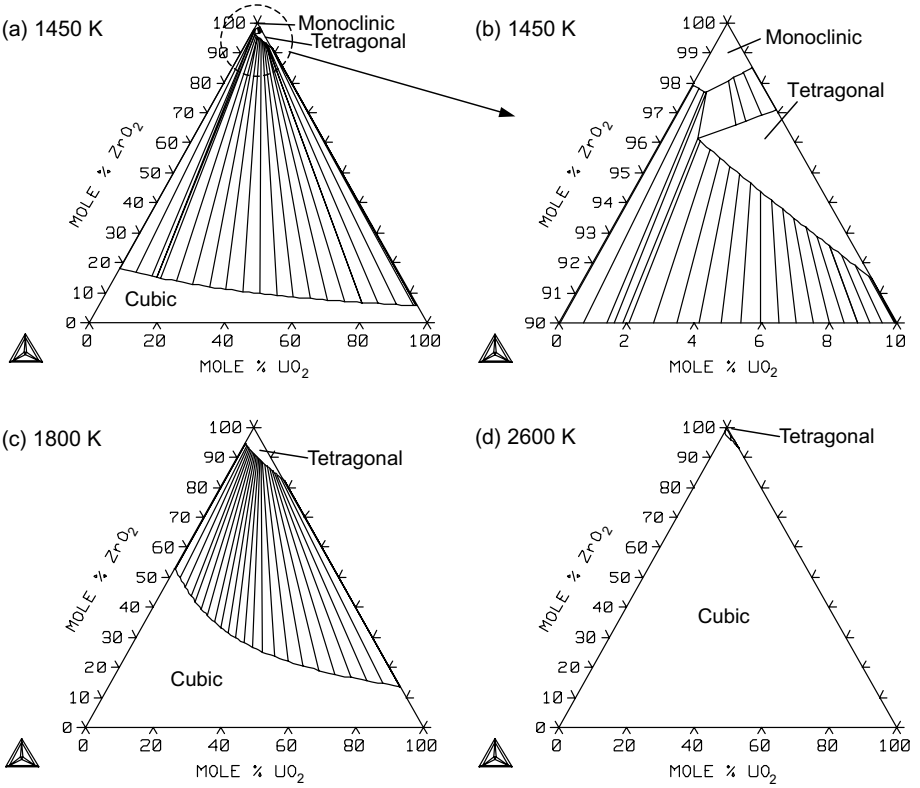

Fig. 3. PuO_2–UO_2–ZrO_2 pseudo-ternary phase diagrams: (a) at 1450 K, (b) at 1450 K, (c) at 1800 K and (d) at 2600 K.

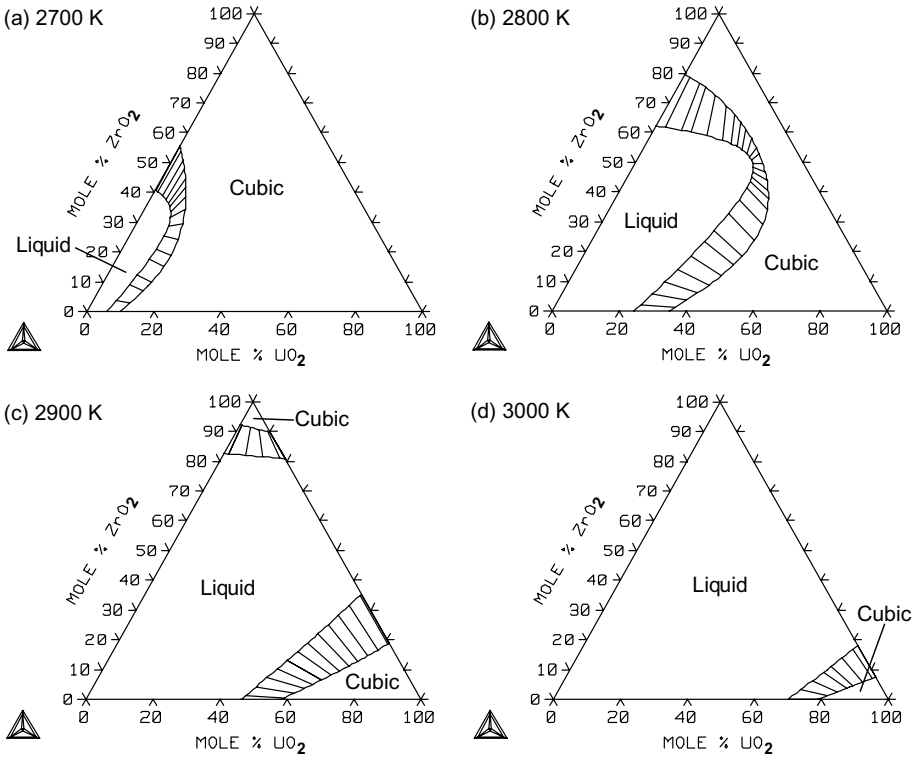

Fig. 4. PuO_2–UO_2–ZrO_2 pseudo-ternary phase diagrams: (a) at 2700 K, (b) at 2800 K, (c) at 2900 K and (d) at 3000 K.

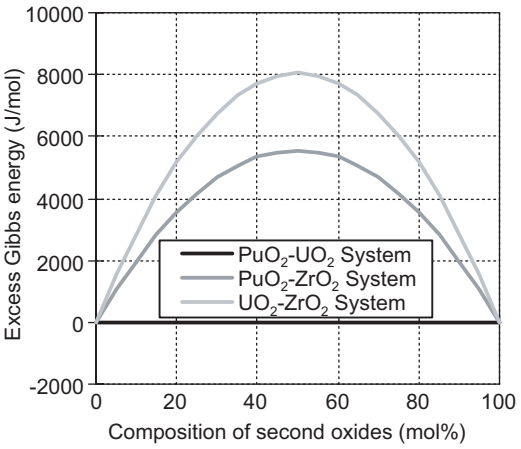

Fig. 5. Excess Gibbs energies of fluorite structure phase for PuO_2–UO_2, PuO_2–ZrO_2 [1] and UO_2–ZrO_2 [2] pseudo-binary systems.

UO_2–ZrO_2 pseudo-binary systems calculated using the interaction parameters adopted in the present study [1,2]. The excess Gibbs energy gives a measure of the deviation from the ideality for solution phases. As can be seen in the figure, the excess Gibbs energies of cubic phases for the PuO_2–ZrO_2 and UO_2–ZrO_2 systems have positive values in the full range of composition. Since the sublattice model of the fluorite structure phase is $(Pu, U, Zr)_1(O)_2$, positive values of the excess Gibbs energy imply a weaker attraction between different cations than the same ones: the average of the Pu–Pu and Zr–Zr interactions (U–U and Zr–Zr interactions) is stronger than the Pu–Zr interaction (U–Zr interaction) in the PuO_2–ZrO_2 system (UO_2–ZrO_2 system). The figure also suggests that this tendency is slightly larger in the UO_2–ZrO_2 system.

Fig. 6 indicates the partial molar enthalpy and entropy of ZrO_2 in the fluorite structure phase of the PuO_2–ZrO_2 and UO_2–ZrO_2 systems at 2600 K for the low ZrO_2 composition region. These quantities reflect the effect of the ZrO_2 on the thermodynamic stability of the fluorite structure phase in the low ZrO_2 composition region. The larger negative value in the partial molar enthalpy and larger positive value in the partial molar entropy indicate that the effect of ZrO_2 dissolution to PuO_2 is larger both on the enthalpy and entropy than that to UO_2. This can be a reason for the higher stability of the fluorite structure phase of the PuO_2–ZrO_2 side in the lower temperature region that implied from the pseudo-ternary phase diagram in the former section.

Fig. 7 indicates the partial molar enthalpy and entropy of PuO_2 and UO_2 in the fluorite structure phase of the PuO_2–ZrO_2 and UO_2–ZrO_2 systems, respectively, at

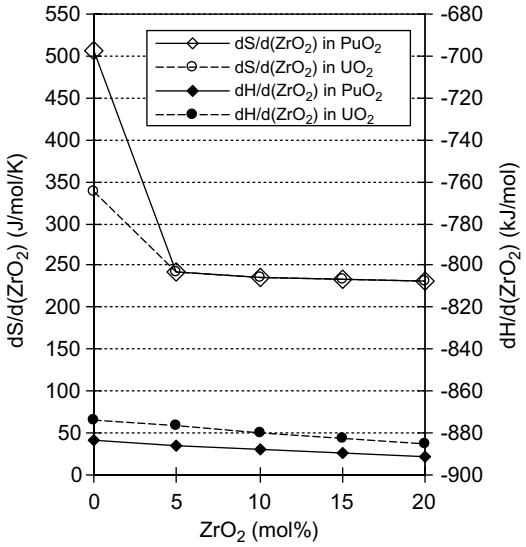

Fig. 6. Partial molar enthalpy and entropy of ZrO_2 in the fluorite structure phase of PuO_2–ZrO_2 and UO_2–ZrO_2 systems at 2600 K for the low ZrO_2 composition region. The $dH/d(ZrO_2)$ and $dS/d(ZrO_2)$ denote partial molar enthalpy and entropy of ZrO_2, respectively.

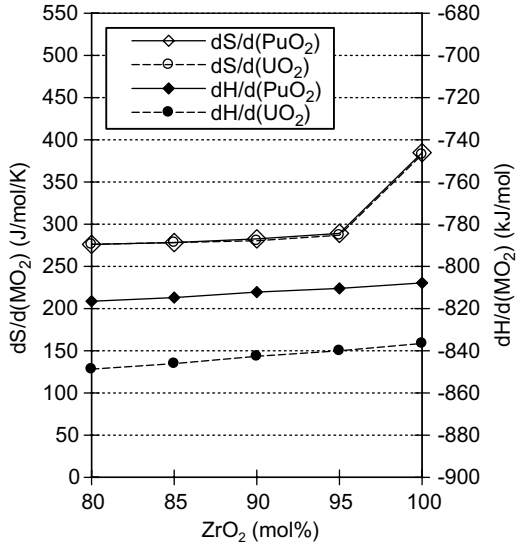

Fig. 7. Partial molar enthalpy and entropy of MO_2 (M = Pu, U) in the fluorite structure phase of PuO_2–ZrO_2 and UO_2–ZrO_2 systems at 2600 K for the high ZrO_2 composition range. The $dH/d(MO_2)$ and $dS/d(MO_2)$ denote partial molar enthalpy and entropy of MO_2, respectively.

2600 K for the high ZrO_2 composition region. Although the effects of PuO_2 and UO_2 dissolution to ZrO_2 are almost identical on the entropy, the effects on the enthalpy are significantly different: the partial molar enthalpy of UO_2 has larger negative values than that of PuO_2. It implies that UO_2 stabilises the fluorite ZrO_2 more than PuO_2. This would explain the higher stability of the fluorite structure phase of the UO_2–ZrO_2 side in the higher temperature region that involves a large portion of ZrO_2 in the composition.

4. Summary

A thermodynamic modelling was performed for PuO_2–UO_2–ZrO_2 system using data available in the literature to evaluate stability of the fluorite structure phase in PuO_2–UO_2–ZrO_2 system.

The assessment of the heat capacity and phase diagram suggested that the deviation from the ideality in the PuO_2–UO_2 system is negligibly small and that it is reasonable to treat the phases in this pseudo-binary system as ideal solutions. The calculated pseudo-ternary phase diagrams implied that the fluorite structure phase of PuO_2–ZrO_2 subsystem is more stable than that of UO_2–ZrO_2 subsystem in the lower temperature range and that the latter is more stable than the former in the higher temperature range.

The effect of ZrO_2 dissolution to PuO_2 was larger both on the enthalpy and entropy of the fluorite structure phase than that to UO_2 in the low ZrO_2 composition range. On the other hand, UO_2 had a larger effect on the stability of the fluorite structure phase in the high ZrO_2 composition range. These results explain well the higher stability of the fluorite structure phase of the PuO_2–ZrO_2 and UO_2–ZrO_2 in the lower and higher temperature regions, respectively, that implied from the pseudo-ternary phase diagrams.

References

[1] H. Kinoshita, M. Uno, S. Yamanaka, J. Alloys Compd. 354 (2003) 129.
[2] M. Yashima, T. Koura, Y. Du, M. Yoshimura, J. Am. Ceram. Soc. 79 (2) (1996) 521.
[3] F. Vettraino, G. Magnani, T. La Torretta, E. Marmo, S. Coelli, L. Luzzi, P. Ossi, G. Zappa, J. Nucl. Mater. 274 (1999) 23.
[4] J.J. Carbajo, G.L. Yoder, S.G. Popov, V.K. Ivanov, J. Nucl. Mater. 299 (2001) 181.
[5] N. Nitani, T. Yamashita, T. Matsuda, S.-i. Kobayashi, T. Ohmichi, J. Nucl. Mater. 274 (1999) 15.
[6] W.L. Gong, W. Lutze, R.C. Ewing, J. Nucl. Mater. 277 (2000) 239.
[7] H. Kleykamp, J. Nucl. Mater. 275 (1999) 1.
[8] N. Saunders, A.P. Miodownik, in: CALPHAD (Calculation of Phase Diagrams): A Comprehensive Guide, Pergamon Materials Series, Vol. 1, Pergamon, Oxford, UK, 1998.

[9] P.Y. Chevalier, E. Fischer, J. Nucl. Mater. 257 (1998) 213.
[10] B. Sundman, Thermo-Calc User's Guide, Royal Institute of Technology, Sweden, 1995.
[11] B. Sundman, J. Agren, J. Phys. Chem. Solids 42 (1981) 297.
[12] O. Redlich, A.T. Kister, Ind. Eng. Chem. 40 (1948) 345.
[13] SGTE Pure Substance Database (Edition 1998), Provided by GTT Technologies, Herzogenrath, Germany, 1998.
[14] R.D. Shannon, Acta. Crystallogr. A 32 (1976) 751.
[15] M. Beauvy, J. Nucl. Mater. 188 (1992) 232.
[16] R.L. Gibby, L. Leibowitz, J.F. Kerrisk, D.G. Clifton, J. Nucl. Mater. 50 (1974) 155.
[17] K. Kurosaki, K. Yamada, M. Uno, S. Yamanaka, K. Yamamoto, T. Namekawa, J. Nucl. Mater. 294 (2001) 160.